ABEP Performance of ISDF Relaying M2M Cooperative Networks

Lingwei Xu[1], Jingjing Wang[1]*, Han Wang [2] and T. Aaron Gulliver[3]
[1] Department of Information Science and Technology, Qingdao University of Science & Technology
Qingdao 266061-China
[e-mail: gaomilaojia2009@163.com]
[e-mail: kathy1003@163.com]
[2] College of Information Science & Technology, Hainan University
Haikou, Hainan 570228-China
[e-mail: : hanwang1214@gmail.com]
[3]Department of Electrical and Computer Engineering, University of Victoria
Victoria V8W 2Y2 - Canada
[e-mail: agullive@ece.uvic.ca]
*Corresponding author: Jingjing Wang

Received May 10, 2016; revised July 24, 2016; accepted August 15, 2016; published December 31, 2016

Abstract

In this paper, the average bit error probability (ABEP) performance of the incremental-selective decode-and-forward (ISDF) relaying mobile-to-mobile (M2M) cooperative networks over *N*-Nakagami fading channels is investigated. The exact ABEP expressions are derived, and the power allocation problem is formulated.The derived ABEP expressions are verified by Monte Carlo simulations. The simulation results showed that the propagation parameters, such as the fading coefficient, and the power-allocation parameter, have a significant influence on the ABEP performance.

Keywords: M2M communication, incremental-selective relaying, decode-and-forward, average bit error probability

This research was supported by National Natural Science Foundation of China (No. 61671261, No. 61304222), the Key Research and Development Program od Shandong Provice (No 2016GGX101007), Shandong Province Outstanding Young Scientist Award Fund (Grant No. 2014BSE28032).

http://dx.doi.org/10.3837/tiis.2016.12.001 **ISSN : 1976-7277**

1. Introduction

In recent years, mobile-to-mobile (M2M) communication is widely employed in various practical application[1, 2]. The emerging heterogeneous mobile network architecture is designed for an increasing amount of traffic, quality requirements, and new mobile cloud computing demands [3]. Due to both sides of the communication are moving, the classical Rayleigh, Rician, or Nakagami fading channels are not applicable to M2M communication.For M2M communication, cascaded fading channels can provide an accurate statistical model by experimental results and theoretical analysis[4-6].The 2-Rayleigh and 2-Nakagami models are considered for the M2M channel in [7,8]. Meijer's G-function is used for the *N*-Nakagami distribution in [9]. The average symbol error probability (ASEP) performance of M2M senor networks over *N*-Nakagami fading channels is investigated in [10]. In the double-antenna switched diversity combining (SDC) system, the ASEP performance over *N*-Nakagami fading channels is investigated in [11].

As a promising solution, cooperative diversity has been employed in mobile M2M communication networks. Using amplify-and-forward (AF) relaying, the bit error rate (BER) of M2M cooperative systems over 2-Nakagami fading channels was investigated in [12]. The end-to-end performance of AF relaying M2M system was investigated in [13]. With incremental decode-and-forward (IDF) relaying, exact average bit error probability (ABEP) expressions for mobile M2M cooperative networks were derived in [14]. Exact ABEP expressions for threshold digital relaying M2M cooperative networks were derived in [15]. The exact closed-form outage probability (OP) expressions were derived for incremental AF(IAF) relaying in [16,17]. The lower bound on OP of M2M cooperative networks was derived for hybrid decode-amplify-forward (HDAF) relaying in [18]. The OP and ASEP performance of M2M cooperative networks with DF relaying were investigated in [19]. The OP performance of M2M cooperative networks with incremental hybrid decode-amplify-forward (IHDAF) relaying were investigated in [20]. The exact closed-form OP expressions were derived for selection incremental relaying in [21]. The lower bound on OP of variable-gain AF relaying was investigated in [22]. The exact closed-form OP expressions were derived for DF relaying in [23].

However, to the best of the authors' knowledge, with incremental-selective decode-and-forward (ISDF) relaying, the ABEP performance of mobile-relay-based M2M cooperative networks over *N*-Nakagami fading channels has not yet been investigated. In [10, 11], we only consider the direct communication, without considering cooperative communication. The performance of cooperative communication is better than that of direct communication. In [14, 15], exact ABEP expressions for IDF relaying and threshold digital relaying are derived. In [16,17,18,20,21,22,23], the OP performance of AF,DF, IAF, HDAF and IHDAF relaying is investigated. In [19], the OP and ASEP performance of DF relaying is investigated.In this paper, the ISDF relaying is considered, which is more complex than DF, IDF, IAF , HDAF and threshold digital relaying. The ABEP analysis is more complex and more valuable than OP and ASEP analysis.Exact ABEP expressions are derived for ISDF relaying over *N*-Nakagami fading channels. The main contributions are listed as follows:

1. We derive exact ABEP expressions for M2M cooperative networks with ISDF relaying.
2. Based on the derived ABEP expressions, the problem of power allocation is solved .

3. Through Monte Carlo simulations,the theoretical analysis is verified. The Results show that the propagation parameters, such as the power allocation parameter, and the fading coefficient have a substantial effect on the ABEP performance.

The rest of the paper is organized as follows. The ISDF relaying M2M cooperative networks model is presented in Section 2. Section 3 provides the exact ABEP expressions for ISDF relaying. The theoretical results are verified by Monte Carlo simulations in Section 4. In Section 5, we conclude the paper.

2. The System Model

The mobile M2M cooperative networks model is depicted in **Fig. 1**, where the mobile source (MS) node communicates with mobile destination (MD) node with the help of the mobile relay (MR) node.They employ a transmitter antenna and a receiver antenna.

According to [12], the distances of MS to MD, MS to MR, and MR to MD links are represented by d_{SD}, d_{SR}, and d_{RD}, respectively. The relative gain of the link between MS to MD is G_{SD}=1.For MS to MR link , and MR to MD link, $G_{SR}=(d_{SD}/d_{SR})^{v}$, $G_{RD} = (d_{SD}/d_{RD})^{v}$, where v is the path loss coefficient [24]. Due to MR is moving, we use the relative geometrical gain μ to indicate the location of MR with respect to MS and MD. We define $\mu= G_{SR}/G_{RD}$ (in decibels) . When MR is midpoint between MS and MD, μ is 1 (0 dB).

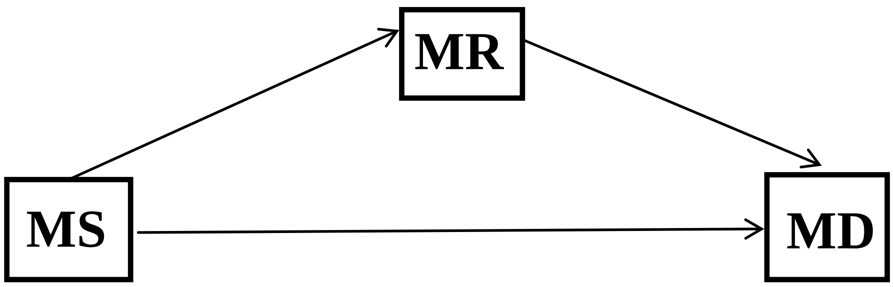

Fig. 1. The system model

$h=h_k$, $k\in\{$SD, SR, RD$\}$, represents the complex channel coefficients of the links in the M2M cooperative networks. h follows N-Nakagami distribution. During the first time slot, the received signals r_{SD} and r_{SR} are given as

$$r_{SD} = \sqrt{KE}h_{SD}x + n_{SD} \tag{1}$$

$$r_{SR} = \sqrt{G_{SR}KE}h_{SR}x + n_{SR} \tag{2}$$

where x denotes the transmitted signal, n_{SR} and n_{SD} are complex Gaussian variables,which have mean 0 and variance $N_0/2$. During the two time slots, E denotes the total energy. K is the power allocation parameter.

During the second time slot, by comparing γ_{SD} to a threshold γ_t, the MR decides whether to activate. γ_{SD} represents the signal-to-noise ratio (SNR) of the link between MS and MD.

If $\gamma_{SD}>\gamma_t$, the MR will not participate in cooperation. The received SNR at MD is given as

$$\gamma_1 = \gamma_{SD} \tag{3}$$

where

$$\gamma_{\mathrm{SD}} = \frac{K\left|h_{\mathrm{SD}}\right|^2 E}{N_0} = K\left|h_{\mathrm{SD}}\right|^2 \bar{\gamma} \tag{4}$$

If $\gamma_{\mathrm{SD}}<\gamma_t$, by comparing γ_{SR} to a threshold γ_p, the MR decides whether to use DF cooperation protocol . γ_{SR} denotes the SNR of the link between MS and MR.

If $\gamma_{\mathrm{SR}}<\gamma_p$, the MR will not participate in cooperation. The received SNR at the MD is given as

$$\gamma_2 = \gamma_{\mathrm{SD}} \tag{5}$$

If $\gamma_{\mathrm{SR}}>\gamma_p$, the MR uses DF cooperation protocol. MR forwards x_1 to the MD. The received signal is given as

$$r_{\mathrm{RD}} = \sqrt{(1-K)G_{\mathrm{RD}}E}\,h_{\mathrm{RD}}x_1 + n_{\mathrm{RD}} \tag{6}$$

where n_{RD} is a complex Gaussian random variable.

To simplify the receiver structure, we use the selection combining (SC) scheme. The received SNR is given as

$$\gamma_{\mathrm{SC}} = \max(\gamma_{\mathrm{SD}}, \gamma_{\mathrm{RD}}) \tag{7}$$

where

$$\gamma_{\mathrm{RD}} = \frac{(1-K)G_{\mathrm{RD}}\left|h_{\mathrm{RD}}\right|^2 E}{N_0} = (1-K)G_{\mathrm{RD}}\left|h_{\mathrm{RD}}\right|^2 \bar{\gamma} \tag{8}$$

h is given by [9]

$$h = \prod_{i=1}^{N} a_i \tag{9}$$

where N is the number of cascaded components, a_i is a Nakagami variable. The probability density function (PDF) of a_i is given as

$$f(a) = \frac{2m^m}{\Omega^m \Gamma(m)} a^{2m-1} \exp(-\frac{m}{\Omega} a^2) \tag{10}$$

m is the fading coefficient, $\Gamma(\cdot)$ is the Gamma function,and Ω is a scaling factor.

The PDF of h is given as [9]

$$f(h) = \frac{2}{h\prod_{i=1}^{N}\Gamma(m_i)} G_{0,N}^{N,0}\left[h^2 \prod_{i=1}^{N} \frac{m_i}{\Omega_i} \Big|_{m_1,\ldots,m_N}^{-} \right] \tag{11}$$

We define $y=|h_k|^2$. The cumulative density function (CDF) of y is [9]

$$F(y) = \frac{1}{\prod_{i=1}^{N}\Gamma(m_i)} G_{1,N+1}^{N,1}\left[y \prod_{i=1}^{N} \frac{m_i}{\Omega_i} \Big|_{m_1,\ldots,m_N,0}^{1} \right] \tag{12}$$

The PDF of y is [9]

$$f(y) = \frac{1}{y\prod_{i=1}^{N}\Gamma(m_i)} G_{0,N}^{N,0}\left[y \prod_{i=1}^{N} \frac{m_i}{\Omega_i} \Big|_{m_1,\ldots,m_N}^{-} \right] \tag{13}$$

3. The ABEP of the ISDF Relaying

The ABEP of the ISDF relaying is given as [25]

$$\begin{aligned} P(\mathrm{e}) = {} & \Pr(\gamma_{\mathrm{SD}} < \gamma_{\mathrm{t}}) \times \Pr(\gamma_{\mathrm{SR}} \geq \gamma_{\mathrm{p}}) \times P_{\mathrm{div}}(\mathrm{e}) + \\ & \Pr(\gamma_{\mathrm{SD}} < \gamma_{\mathrm{t}}) \times \Pr(\gamma_{\mathrm{SR}} < \gamma_{\mathrm{p}}) \times P_{\mathrm{direct1}}(\mathrm{e}) + \\ & \Pr(\gamma_{\mathrm{SD}} \geq \gamma_{\mathrm{t}}) \times P_{\mathrm{direct2}}(\mathrm{e}) \end{aligned} \tag{14}$$

where $P_{\mathrm{div}}(\mathrm{e})$ is the error rate at MD after combining the signals from MR and MS given that MR transmits its received signal. $P_{\mathrm{direct1}}(\mathrm{e})$ is the error rate at MD when MR is requested to forward signal but decides not to forward due to the poor quality of its received signal. $P_{\mathrm{direct2}}(\mathrm{e})$ is the error rate when MR needn't participate in cooperation.

The CDF of γ_{SD} is given as

$$F_{\gamma_{\mathrm{SD}}}(r) = \frac{1}{\prod_{i=1}^{N} \Gamma(m_i)} G_{1,N+1}^{N,1}\left[\frac{r}{\overline{\gamma_{\mathrm{SD}}}} \prod_{i=1}^{N} \frac{m_i}{\Omega_i} \Big|_{m_1,\ldots,m_N,0}^{1} \right] \tag{15}$$

where

$$\overline{\gamma_{\mathrm{SD}}} = K\bar{\gamma} \tag{16}$$

The CDF of γ_{SR} is given as

$$F_{\gamma_{\mathrm{SR}}}(r) = \frac{1}{\prod_{j=1}^{N} \Gamma(m_j)} G_{1,N+1}^{N,1}\left[\frac{r}{\overline{\gamma_{\mathrm{SR}}}} \prod_{j=1}^{N} \frac{m_j}{\Omega_j} \Big|_{m_1,\ldots,m_N,0}^{1} \right] \tag{17}$$

where

$$\overline{\gamma_{\mathrm{SR}}} = KG_{\mathrm{SR}}\bar{\gamma} \tag{18}$$

So we can obtain

$$\Pr(\gamma_{\mathrm{SD}} < \gamma_{\mathrm{t}}) = \frac{1}{\prod_{i=1}^{N} \Gamma(m_i)} G_{1,N+1}^{N,1}\left[\frac{\gamma_{\mathrm{t}}}{\overline{\gamma_{\mathrm{SD}}}} \prod_{i=1}^{N} \frac{m_i}{\Omega_i} \Big|_{m_1,\ldots,m_N,0}^{1} \right] \tag{19}$$

$$\Pr(\gamma_{\mathrm{SR}} < \gamma_{\mathrm{p}}) = \frac{1}{\prod_{t=1}^{N} \Gamma(m_t)} G_{1,N+1}^{N,1}\left[\frac{\gamma_{\mathrm{p}}}{\overline{\gamma_{\mathrm{SR}}}} \prod_{t=1}^{N} \frac{m_t}{\Omega_t} \Big|_{m_1,\ldots,m_N,0}^{1} \right] \tag{20}$$

Next, the $P_{\mathrm{direct2}}(\mathrm{e})$ is evaluated. The $P_{\mathrm{direct2}}(\mathrm{e})$ is given as

$$P_{\mathrm{direct2}}(\mathrm{e}) = \int_0^{\infty} P(e|r) f_{\gamma_{\mathrm{SD}}}(r|\gamma_{\mathrm{SD}} \geq \gamma_{\mathrm{t}}) dr \tag{21}$$

where

$$P(\mathrm{e}|r) = a \times erfc(\sqrt{br}) \tag{22}$$

For BPSK: $a = 0.5$ and $b = 1$, QPSK: $a = 0.5$ and $b = 0.5$.

$$f_{\gamma_{\mathrm{SD}}}(r|\gamma_{\mathrm{SD}} \geq \gamma_{\mathrm{t}}) =$$
$$\begin{cases} 0, & r \leq \gamma_{\mathrm{t}} \\ \dfrac{\dfrac{1}{r\prod_{i=1}^{N}\Gamma(m_i)} G_{0,N}^{N,0}\left[\dfrac{r}{\gamma_{\mathrm{SD}}}\prod_{i=1}^{N}\dfrac{m_i}{\Omega_i}\Big|_{m_1,\ldots,m_N}^{-}\right]}{1-\dfrac{1}{\prod_{i=1}^{N}\Gamma(m_i)} G_{1,N+1}^{N,1}\left[\dfrac{\gamma_{\mathrm{t}}}{\gamma_{\mathrm{SD}}}\prod_{i=1}^{N}\dfrac{m_i}{\Omega_i}\Big|_{m_1,\ldots,m_N,0}^{1}\right]}, & r > \gamma_{\mathrm{t}} \end{cases}$$
$$= \begin{cases} 0, & r \leq \gamma_{\mathrm{t}} \\ \dfrac{\dfrac{1}{r} G_{0,N}^{N,0}\left[\dfrac{r}{\gamma_{\mathrm{SD}}}\prod_{i=1}^{N}\dfrac{m_i}{\Omega_i}\Big|_{m_1,\ldots,m_N}^{-}\right]}{\prod_{i=1}^{N}\Gamma(m_i) - G_{1,N+1}^{N,1}\left[\dfrac{\gamma_{\mathrm{t}}}{\gamma_{\mathrm{SD}}}\prod_{i=1}^{N}\dfrac{m_i}{\Omega_i}\Big|_{m_1,\ldots,m_N,0}^{1}\right]}, & r > \gamma_{\mathrm{t}} \end{cases} \tag{23}$$

Combining (22) and (23), the $P_{\mathrm{direct2}}(\mathrm{e})$ is given as

$$\begin{aligned} P_{\mathrm{direct2}}(\mathrm{e}) &= \frac{a}{\prod_{i=1}^{N}\Gamma(m_i) - G_{1,N+1}^{N,1}\left[\dfrac{\gamma_{\mathrm{t}}}{\gamma_{\mathrm{SD}}}\prod_{i=1}^{N}\dfrac{m_i}{\Omega_i}\Big|_{m_1,\ldots,m_N,0}^{1}\right]} \times \\ &\int_{\gamma_{\mathrm{t}}}^{\infty} erfc(\sqrt{br})\frac{1}{r}G_{0,N}^{N,0}\left[\frac{r}{\gamma_{\mathrm{SD}}}\prod_{i=1}^{N}\frac{m_i}{\Omega_i}\Big|_{m_1,\ldots,m_N}^{-}\right]dr \\ &= \frac{a}{\prod_{i=1}^{N}\Gamma(m_i) - G_{1,N+1}^{N,1}\left[\dfrac{\gamma_{\mathrm{t}}}{\gamma_{\mathrm{SD}}}\prod_{i=1}^{N}\dfrac{m_i}{\Omega_i}\Big|_{m_1,\ldots,m_N,0}^{1}\right]} \times \\ &\left[\begin{array}{l} \int_{0}^{\infty} erfc(\sqrt{br})\frac{1}{r}G_{0,N}^{N,0}\left[\frac{r}{\gamma_{\mathrm{SD}}}\prod_{i=1}^{N}\frac{m_i}{\Omega_i}\Big|_{m_1,\ldots,m_N}^{-}\right]dr - \\ \int_{0}^{\gamma_{\mathrm{t}}} erfc(\sqrt{br})\frac{1}{r}G_{0,N}^{N,0}\left[\frac{r}{\gamma_{\mathrm{SD}}}\prod_{i=1}^{N}\frac{m_i}{\Omega_i}\Big|_{m_1,\ldots,m_N}^{-}\right]dr \end{array}\right] \\ &= \frac{a}{\prod_{i=1}^{N}\Gamma(m_i) - G_{1,N+1}^{N,1}\left[\dfrac{\gamma_{\mathrm{t}}}{\gamma_{\mathrm{SD}}}\prod_{i=1}^{N}\dfrac{m_i}{\Omega_i}\Big|_{m_1,\ldots,m_N,0}^{1}\right]}\left[G_1 - G_2\right] \end{aligned} \tag{24}$$

With the help of [26], the G_1 is given as

$$\begin{aligned} G_1 &= \int_0^{\infty} erfc(\sqrt{br})\frac{1}{r}G_{0,N}^{N,0}\left[\frac{r}{\overline{\gamma}_{SD}}\prod_{i=1}^{N}\frac{m_i}{\Omega_i}\bigg|_{m_1,....,m_N}^{-}\right]dr \\ &= \frac{1}{\sqrt{\pi}}\int_0^{\infty} r^{-1}G_{1,2}^{2,0}\left(br\bigg|_{0,\frac{1}{2}}^{1}\right)G_{0,N}^{N,0}\left[\frac{r}{\overline{\gamma}_{SD}}\prod_{i=1}^{N}\frac{m_i}{\Omega_i}\bigg|_{m_1,....,m_N}^{-}\right]dr \\ &= \frac{1}{\sqrt{\pi}}G_{2,N+1}^{N,2}\left[\frac{1}{b\overline{\gamma}_{SD}}\prod_{i=1}^{N}\frac{m_i}{\Omega_i}\bigg|_{m_1,....,m_N,0}^{1,\frac{1}{2}}\right] \end{aligned} \tag{25}$$

Next, the G_2 is given as

$$\begin{aligned} G_2 &= \int_0^{\gamma_t} erfc(\sqrt{br})\frac{1}{r}G_{0,N}^{N,0}\left[\frac{r}{\overline{\gamma}_{SD}}\prod_{i=1}^{N}\frac{m_i}{\Omega_i}\bigg|_{m_1,....,m_N}^{-}\right]dr \\ &= \frac{1}{\sqrt{\pi}}\int_0^{\gamma_t} r^{-1}G_{1,2}^{2,0}\left(br\bigg|_{0,\frac{1}{2}}^{1}\right)G_{0,N}^{N,0}\left[\frac{r}{\overline{\gamma}_{SD}}\prod_{i=1}^{N}\frac{m_i}{\Omega_i}\bigg|_{m_1,....,m_N}^{-}\right]dr \end{aligned} \tag{26}$$

We can rewritten the Meijer's G-function as [27]

$$\begin{aligned} &G_{1,2}^{2,0}\left[br\bigg|_{0,\frac{1}{2}}^{1}\right] \\ &= \Gamma(\frac{1}{2})\,{}_1F_1(0;1,\frac{1}{2};-br) + \frac{\Gamma(-\frac{1}{2})}{\Gamma(\frac{1}{2})}(br)^{\frac{1}{2}}\,{}_1F_1(\frac{1}{2};\frac{3}{2},1;-br) \\ &= \sqrt{\pi} + \frac{\Gamma(-\frac{1}{2})}{\sqrt{\pi}}\sum_{k=0}^{\infty}\frac{(\frac{1}{2})_k(-1)^k(b)^{k+\frac{1}{2}}}{(\frac{3}{2})_k k!}\frac{r^{k+\frac{1}{2}}}{k!} \end{aligned} \tag{27}$$

$$\begin{aligned} &{}_pF_q(\alpha_1,\alpha_2,....,\alpha_p;\beta_1,\beta_2,....,\beta_q;z) \\ &= \sum_{k=0}^{\infty}\frac{(\alpha_1)_k(\alpha_2)_k....(\alpha_p)_k}{(\beta_1)_k(\beta_2)_k....(\beta_q)_k}\frac{z^k}{k!} \end{aligned} \tag{28}$$

$$(x)_k = \prod_{t=0}^{k-1}(x+t), (x)_0 = 1 \tag{29}$$

The G_2 is given as

$$G_2 = \int_0^{\gamma_{\mathrm{t}}} r^{-1} G_{0,N}^{N,0}\left[\frac{r}{\overline{\gamma}_{\mathrm{SD}}}\prod_{i=1}^{N}\frac{m_i}{\Omega_i}\Big|_{m_1,\ldots,m_N}^{-}\right]dr$$
$$+\frac{\Gamma(-\frac{1}{2})}{\pi}\times\sum_{k=0}^{\infty}\frac{(\frac{1}{2})_k(-1)^k(b)^{k+\frac{1}{2}}}{(\frac{3}{2})_k(k!)^2}\times$$
$$\int_0^{\gamma_{\mathrm{t}}} r^{k-\frac{1}{2}} G_{0,N}^{N,0}\left[\frac{r}{\overline{\gamma}_{\mathrm{SD}}}\prod_{i=1}^{N}\frac{m_i}{\Omega_i}\Big|_{m_1,\ldots,m_N}^{-}\right]dr$$
$$= G_{1,N+1}^{N,1}\left[\frac{\gamma_{\mathrm{t}}}{\overline{\gamma}_{\mathrm{SD}}}\prod_{i=1}^{N}\frac{m_i}{\Omega_i}\Big|_{m_1,\ldots,m_N,0}^{1}\right]+\frac{\Gamma(-\frac{1}{2})}{\pi}\times$$
$$\sum_{k=0}^{\infty}\frac{(\frac{1}{2})_k(-1)^k(b)^{k+\frac{1}{2}}}{(\frac{3}{2})_k(k!)^2} G_{1,N+1}^{N,1}\left[\frac{\gamma_{\mathrm{t}}}{\overline{\gamma}_{\mathrm{SD}}}\prod_{i=1}^{N}\frac{m_i}{\Omega_i}\Big|_{m_1,\ldots,m_N,-k-\frac{1}{2}}^{\frac{1}{2}-k}\right] \tag{30}$$

Next, the $P_{\mathrm{direct1}}(\mathrm{e})$ is given as

$$P_{\mathrm{direct1}}(\mathrm{e}) = \int_0^{\infty} P(\mathrm{e}|\mathrm{r}) f_{\gamma_{\mathrm{SD}}}(r|\gamma_{\mathrm{SD}} < \gamma_{\mathrm{t}})dr \tag{31}$$

where

$$f_{\gamma_{\mathrm{SD}}}(r|\gamma_{\mathrm{SD}} < \gamma_{\mathrm{t}}) =$$
$$= \begin{cases} \dfrac{\frac{1}{r}G_{0,N}^{N,0}\left[\frac{r}{\overline{\gamma}_{\mathrm{SD}}}\prod_{i=1}^{N}\frac{m_i}{\Omega_i}\Big|_{m_1,\ldots,m_N}^{-}\right]}{G_{1,N+1}^{N,1}\left[\frac{\gamma_{\mathrm{t}}}{\overline{\gamma}_{\mathrm{SD}}}\prod_{i=1}^{N}\frac{m_i}{\Omega_i}\Big|_{m_1,\ldots,m_N,0}^{1}\right]}, & r \le \gamma_{\mathrm{t}} \\ 0, & r > \gamma_{\mathrm{t}} \end{cases} \tag{32}$$

Combining (22) and (32), the $P_{\mathrm{direct1}}(\mathrm{e})$ is expressed as

$$
\begin{aligned}
P_{\text{direct1}}(\text{e}) &= a\int_0^{\infty} erfc(\sqrt{br})\, f_{\gamma_{\text{SD}}}(r \mid \gamma_{\text{SD}} < \gamma_{\text{t}})dr \\
&= \frac{a}{G_{1,N+1}^{N,1}\left[\frac{\gamma_{\text{t}}}{\gamma_{\text{SD}}}\prod_{i=1}^{N}\frac{m_i}{\Omega_i}\Big|_{m_1,\ldots,m_N,0}^{1}\right]}\times \\
&\int_0^{\gamma_{\text{t}}} erfc(\sqrt{br})\frac{1}{r}G_{0,N}^{N,0}\left[\frac{r}{\gamma_{\text{SD}}}\prod_{i=1}^{N}\frac{m_i}{\Omega_i}\Big|_{m_1,\ldots,m_N}^{-}\right]dr \\
&= \frac{a}{G_{1,N+1}^{N,1}\left[\frac{\gamma_{\text{t}}}{\gamma_{\text{SD}}}\prod_{i=1}^{N}\frac{m_i}{\Omega_i}\Big|_{m_1,\ldots,m_N,0}^{1}\right]}G_2
\end{aligned}
\tag{33}
$$

Next, the $P_{\text{div}}(\text{e})$ is given as

$$
P_{\text{div}}(\text{e}) = P_{\text{SR}}(\text{e})P_{\text{x}}(\text{e}) + (1 - P_{\text{SR}}(\text{e}))P_{\text{com}}(\text{e}) \tag{34}
$$

where $P_{\text{SR}}(\text{e})$ is the error rate at MR, $P_{\text{x}}(\text{e})$ is the error rate at MD given that MR decoded unsuccessfully, and $P_{\text{com}}(\text{e})$ is the error rate at MD given that MR decoded correctly.

The $P_{\text{SR}}(\text{e})$ is given as

$$
P_{\text{SR}}(\text{e}) = \int_0^{\infty} P(\text{e}\mid\text{r}) f_{\gamma_{\text{SR}}}(r \mid \gamma_{\text{SR}} > \gamma_{\text{p}})dr \tag{35}
$$

where

$$
f_{\gamma_{\text{SR}}}(r \mid \gamma_{\text{SR}} > \gamma_{\text{p}}) =
\begin{cases}
0, & r \le \gamma_{\text{p}} \\
\dfrac{\frac{1}{r}G_{0,N}^{N,0}\left[\frac{r}{\gamma_{\text{SR}}}\prod_{t=1}^{N}\frac{m_t}{\Omega_t}\Big|_{m_1,\ldots,m_N}^{-}\right]}{\prod_{t=1}^{N}\Gamma(m_t) - G_{1,N+1}^{N,1}\left[\frac{\gamma_{\text{p}}}{\gamma_{\text{SR}}}\prod_{t=1}^{N}\frac{m_t}{\Omega_t}\Big|_{m_1,\ldots,m_N,0}^{1}\right]}, & r > \gamma_{\text{p}}
\end{cases}
\tag{36}
$$

Combining (22) and (36), the $P_{\text{SR}}(\text{e})$ is expressed as

$$\begin{aligned} P_{\mathrm{SR}}(\mathrm{e}) &= \frac{a}{\prod_{t=1}^{N}\Gamma(m_t) - G_{1,N+1}^{N,1}\left[\frac{\gamma_{\mathrm{p}}}{\gamma_{\mathrm{SR}}}\prod_{t=1}^{N}\frac{m_t}{\Omega_t}\Big|_{m_1,\ldots,m_N,0}^{1}\right]}\times \\ &\int_{\gamma_{\mathrm{p}}}^{\infty} erfc(\sqrt{br})\frac{1}{r}G_{0,N}^{N,0}\left[\frac{r}{\gamma_{\mathrm{SR}}}\prod_{t=1}^{N}\frac{m_t}{\Omega_t}\Big|_{m_1,\ldots,m_N}^{-}\right]dr \\ &= \frac{a}{\prod_{t=1}^{N}\Gamma(m_t) - G_{1,N+1}^{N,1}\left[\frac{\gamma_{\mathrm{p}}}{\gamma_{\mathrm{SR}}}\prod_{t=1}^{N}\frac{m_t}{\Omega_t}\Big|_{m_1,\ldots,m_N,0}^{1}\right]}\times \\ &\left(\frac{1}{\sqrt{\pi}}G_{2,N+1}^{N,2}\left[\frac{1}{b\gamma_{\mathrm{SR}}}\prod_{t=1}^{N}\frac{m_t}{\Omega_t}\Big|_{m_1,\ldots,m_N,0}^{1,\frac{1}{2}}\right] - GG\right) \end{aligned} \tag{37}$$

where

$$\begin{aligned} GG &= \int_{0}^{\gamma_{\mathrm{p}}} erfc(\sqrt{br})\frac{1}{r}G_{0,N}^{N,0}\left[\frac{r}{\gamma_{\mathrm{SR}}}\prod_{t=1}^{N}\frac{m_t}{\Omega_t}\Big|_{m_1,\ldots,m_N}^{-}\right]dr \\ &= G_{1,N+1}^{N,1}\left[\frac{\gamma_{\mathrm{p}}}{\gamma_{\mathrm{SR}}}\prod_{t=1}^{N}\frac{m_t}{\Omega_t}\Big|_{m_1,\ldots,m_N,0}^{1}\right] + \frac{\Gamma(-\frac{1}{2})}{\pi}\times \\ &\sum_{k=0}^{\infty}\frac{(\frac{1}{2})_k(-1)^k(b)^{k+\frac{1}{2}}}{(\frac{3}{2})_k(k!)^2}G_{1,N+1}^{N,1}\left[\frac{\gamma_{\mathrm{p}}}{\gamma_{\mathrm{SR}}}\prod_{t=1}^{N}\frac{m_t}{\Omega_t}\Big|_{m_1,\ldots,m_N,-k-\frac{1}{2}}^{\frac{1}{2}-k}\right] \end{aligned} \tag{38}$$

When MR makes an incorrect detection and forwards an erroneous signal to MD, with reference to [28], the P_{x} (e) can be derived as

$$\begin{aligned} P_{\mathrm{x}}(\mathrm{e}) &= \int_0^{\infty}\int_0^{\gamma_2} f_{\gamma_{\mathrm{SD}}}(\gamma_1|\gamma_{\mathrm{SD}}<\gamma_{\mathrm{t}}) f_{\gamma_{\mathrm{RD}}}(\gamma_2)d\gamma_1 d\gamma_2 \\ &+ a\int_0^{\infty}\int_{\gamma_2}^{\infty} erfc(\sqrt{b\gamma_1}) f_{\gamma_{\mathrm{SD}}}(\gamma_1|\gamma_{\mathrm{SD}}<\gamma_{\mathrm{t}}) f_{\gamma_{RD}}(\gamma_2)d\gamma_1 d\gamma_2 \\ &= G_3 + aG_4 \end{aligned} \tag{39}$$

Next, the G_3 is given as

$$
\begin{aligned}
G_3 &= \frac{1}{F_{\gamma_{\mathrm{SD}}}(\gamma_{\mathrm{t}})}\int_0^{\gamma_{\mathrm{t}}}\int_0^{\gamma_2} f_{\gamma_{\mathrm{SD}}}(\gamma_1) f_{\gamma_{\mathrm{RD}}}(\gamma_2) d\gamma_1 d\gamma_2 \\
&+ \frac{1}{F_{\gamma_{\mathrm{SD}}}(\gamma_{\mathrm{t}})}\int_{\gamma_{\mathrm{t}}}^{\infty}\int_0^{\gamma_{\mathrm{t}}} f_{\gamma_{\mathrm{SD}}}(\gamma_1) f_{\gamma_{\mathrm{RD}}}(\gamma_2) d\gamma_1 d\gamma_2 \\
&= \frac{1}{F_{\gamma_{\mathrm{SD}}}(\gamma_{\mathrm{t}})}\int_0^{\gamma_{\mathrm{t}}} F_{\gamma_{\mathrm{SD}}}(\gamma_2) f_{\gamma_{\mathrm{RD}}}(\gamma_2) d\gamma_2 + \\
&\quad (1 - F_{\gamma_{\mathrm{RD}}}(\gamma_{\mathrm{t}})) \\
&= \frac{1}{F_{\gamma_{\mathrm{SD}}}(\gamma_{\mathrm{t}})} G_5 + (1 - F_{\gamma_{\mathrm{RD}}}(\gamma_{\mathrm{t}}))
\end{aligned} \tag{40}
$$

where

$$
\begin{aligned}
G_5 &= \frac{1}{\prod_{i=1}^{N}\Gamma(m_i)\prod_{tt=1}^{N}\Gamma(m_{tt})}\sum_{g=1}^{N}\frac{\prod_{j=1}^{N}\Gamma(m_j - m_g)\Gamma(m_g)}{\Gamma(1+m_g)} \\
&\times\sum_{k=0}^{\infty}\frac{(-1)^{Nk}\left(\frac{1}{\overline{\gamma_{\mathrm{SD}}}}\prod_{i=1}^{N}\frac{m_i}{\Omega_i}\right)^{k+m_g}(m_g)_k}{(1+m_g-m_1)_k(1+m_g-m_2)_k\ldots.(1+m_g)_k}\frac{1}{k!} \\
&\times(\gamma_{\mathrm{t}})^{k+m_g} G_{1,N+1}^{N,1}\left[\frac{\gamma_{\mathrm{t}}}{\overline{\gamma_{\mathrm{RD}}}}\prod_{tt=1}^{N}\frac{m_{tt}}{\Omega_{tt}}\middle|\begin{matrix}1-k-m_g\\ m_1,\ldots.,m_N,-k-m_g\end{matrix}\right]
\end{aligned} \tag{41}
$$

$$
F_{\gamma_{\mathrm{SD}}}(\gamma_{\mathrm{t}}) = \frac{1}{\prod_{i=1}^{N}\Gamma(m_i)} G_{1,N+1}^{N,1}\left[\frac{\gamma_{\mathrm{t}}}{\overline{\gamma_{\mathrm{SD}}}}\prod_{i=1}^{N}\frac{m_i}{\Omega_i}\middle|\begin{matrix}1\\ m_1,\ldots.,m_N,0\end{matrix}\right] \tag{42}
$$

$$
F_{\gamma_{\mathrm{RD}}}(\gamma_{\mathrm{t}}) = \frac{1}{\prod_{tt=1}^{N}\Gamma(m_{tt})} G_{1,N+1}^{N,1}\left[\frac{\gamma_{\mathrm{t}}}{\overline{\gamma_{\mathrm{RD}}}}\prod_{tt=1}^{N}\frac{m_{tt}}{\Omega_{tt}}\middle|\begin{matrix}1\\ m_1,\ldots.,m_N,0\end{matrix}\right] \tag{43}
$$

$$
\overline{\gamma_{\mathrm{RD}}} = (1-K) G_{\mathrm{RD}}\bar{\gamma} \tag{44}
$$

Next, the G_4 is given as

$$G_4 = \frac{1}{F_{\gamma_{SD}}(\gamma_t)} \int_0^{\gamma_t} \int_{\gamma_2}^{\gamma_t} erfc(\sqrt{b\gamma_1}) f_{\gamma_{SD}}(\gamma_1) f_{\gamma_{RD}}(\gamma_2) d\gamma_1 d\gamma_2$$

$$= \frac{1}{F_{\gamma_{SD}}(\gamma_t) \prod_{i=1}^{N} \Gamma(m_i) \prod_{tt=1}^{N} \Gamma(m_{tt})} \times \tag{45}$$

$$\left(G_2 F_{\gamma_{RD}}(\gamma_t) - G_5 - \frac{\Gamma(-\frac{1}{2})}{\pi} \sum_{k=0}^{\infty} \frac{(\frac{1}{2})_k (-1)^k (b)^{k+\frac{1}{2}}}{(\frac{3}{2})_k (k!)^2} G_{55} \right)$$

$$G_{55} = \sum_{g=1}^{N} \frac{\prod_{j=1}^{N} \Gamma(m_j - m_g) \Gamma(m_g)}{\Gamma(1+m_g)}$$

$$\times \sum_{k=0}^{\infty} \frac{(-1)^{Nk} (\frac{1}{\overline{\gamma}_{SD}} \prod_{i=1}^{N} \frac{m_i}{\Omega_i})^{k+m_g} (m_g)_k}{(1+m_g-m_1)_k (1+m_g-m_2)_k \ldots . (1+m_g)_k} \frac{1}{k!} \tag{46}$$

$$\times (\gamma_t)^{k+m_g} G_{1,N+1}^{N,1} \left[\frac{\gamma_t}{\overline{\gamma}_{RD}} \prod_{tt=1}^{N} \frac{m_{tt}}{\Omega_{tt}} \middle| \begin{matrix} \frac{1}{2}+k \\ m_1, \ldots, m_N, -k-m_g \end{matrix} \right]$$

The $P_{com}(e)$ is given as

$$P_{com}(e) = a \int_0^{\infty} erfc(\sqrt{br}) f_{\gamma_{SC}}(r | \gamma_{SD} < \gamma_t) dr \tag{47}$$

where

$$f_{\gamma_{SC}}(r | \gamma_{SD} < \gamma_t) = \begin{cases} \frac{1}{F_{\gamma_{SD}}(\gamma_t)} \left(f_{\gamma_{SD}}(r) F_{\gamma_{RD}}(r) + F_{\gamma_{SD}}(r) f_{\gamma_{RD}}(r) \right), r \le \gamma_t \\ f_{\gamma_{RD}}(r), \qquad r > \gamma_t \end{cases} \tag{48}$$

Combining (47) and (48), the $P_{com}(e)$ is given as

$$P_{com}(e) = \frac{a}{F_{\gamma_{SD}}(\gamma_t)} \times \left(\int_0^{\gamma_t} erfc(\sqrt{br}) f_{\gamma_{SD}}(r) F_{\gamma_{RD}}(r) dr + \right.$$

$$\left. \int_0^{\gamma_t} erfc(\sqrt{br}) F_{\gamma_{SD}}(r) f_{\gamma_{RD}}(r) dr \right) + a \int_{\gamma_t}^{\infty} erfc(\sqrt{br}) f_{\gamma_{RD}}(r) dr \tag{49}$$

$$= a \left[\frac{1}{F_{\gamma_{SD}}(\gamma_t)} \left(G_6 + G_7 \right) + G_8 \right]$$

Next, the G_8 is evaluated.

$$G_8 = \frac{1}{\prod_{tt=1}^{N}\Gamma(m_{tt})}\int_0^{\infty}\frac{1}{r}erfc(\sqrt{br})G_{0,N}^{N,0}\left[\frac{r}{\gamma_{\mathrm{RD}}}\prod_{tt=1}^{N}\frac{m_{tt}}{\Omega_{tt}}\Big|_{m_1,\ldots,m_N}^{-}\right]dr$$
$$-\frac{1}{\prod_{tt=1}^{N}\Gamma(m_{tt})}\int_0^{\gamma_t}\frac{1}{r}erfc(\sqrt{br})G_{0,N}^{N,0}\left[\frac{r}{\gamma_{\mathrm{RD}}}\prod_{tt=1}^{N}\frac{m_{tt}}{\Omega_{tt}}\Big|_{m_1,\ldots,m_N}^{-}\right]dr \quad (50)$$
$$=\frac{1}{\prod_{tt=1}^{N}\Gamma(m_{tt})}\left(\frac{1}{\sqrt{\pi}}G_{2,N+1}^{N,2}\left[\frac{1}{b\gamma_{\mathrm{RD}}}\prod_{tt=1}^{N}\frac{m_{tt}}{\Omega_{tt}}\Big|_{m_1,\ldots,m_N,0}^{1,\frac{1}{2}}\right]-G_9\right)$$

$$G_9 = G_{1,N+1}^{N,1}\left[\frac{\gamma_t}{\gamma_{\mathrm{RD}}}\prod_{tt=1}^{N}\frac{m_{tt}}{\Omega_{tt}}\Big|_{m_1,\ldots,m_N,0}^{1}\right]+\frac{\Gamma(-\frac{1}{2})}{\pi}\times$$
$$\sum_{k=0}^{\infty}\frac{(\frac{1}{2})_k(-1)^k(b)^{k+\frac{1}{2}}}{(\frac{3}{2})_k(k!)^2}G_{1,N+1}^{N,1}\left[\frac{\gamma_t}{\gamma_{\mathrm{RD}}}\prod_{tt=1}^{N}\frac{m_{tt}}{\Omega_{tt}}\Big|_{m_1,\ldots,m_N,-k-\frac{1}{2}}^{\frac{1}{2}-k}\right] \quad (51)$$

G_6, G_7 can be evaluated by using common mathematical software packages, such as MATHEMATICA or MAPLE.

4. Experimental Results and Analysis

In this section, through Monte Carlo simulations, we confirm the derived theoretical results. BPSK modulation is used to obtain the simulation results.

Table 1. The parameters for different scenarios

	Scenario 1	Scenario 2	Scenario 3
m_{SD}	1	1	2
m_{SR}	1	1	2
m_{RD}	1	1	2
N_{SD}	3	2	2
N_{SR}	2	2	2
N_{RD}	2	2	2

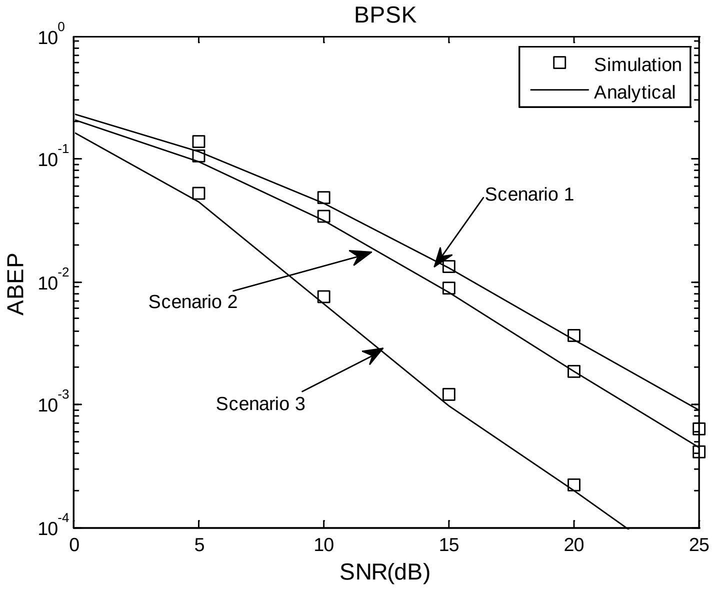

Fig. 2. The ABEP performance over *N*-Nakagami fading channels

In **Fig. 2**, we compare the simulation and theoretical results. The parameters are μ=0 dB, K=0.5. The given threshold is γ_t =4 dB, γ_p=2 dB. In **Table 1**, we present the combinations of N and m.From **Fig. 2**, it shows that the simulation results coincide with the theoretical results well. It verifies the accuracy of the theoretical results. The ABEP performance is improved with the SNR increased. For example, in Scenario 2, when SNR=10 dB, the ABEP is 1×10^{-1}, SNR=12 dB, the ABEP is 7.5×10^{-2}.

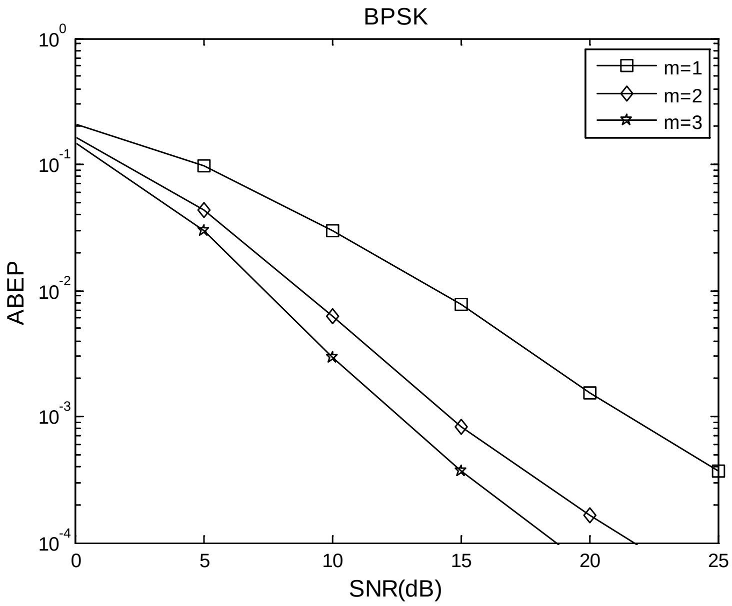

Fig. 3. The ABEP performance versus *m*

Fig. 3 presents the ABEP performance versus m . The parameters are N=2, m=1, 2, 3, μ=0 dB, γ_t=4 dB, γ_p=2 dB, K=0.6. In **Fig. 3**, with m increased, we can obtain that the ABEP performance is improved . For example, when SNR=10 dB, m=1, the ABEP is 3.5×10^{-2}, m=2, the ABEP is 7×10^{-3}, m=3, the ABEP is 3.8×10^{-3}. Increasing m means that the fading severity of the cascaded channels decreases. With m fixed, increasing the SNR reduces the ABEP gradually.

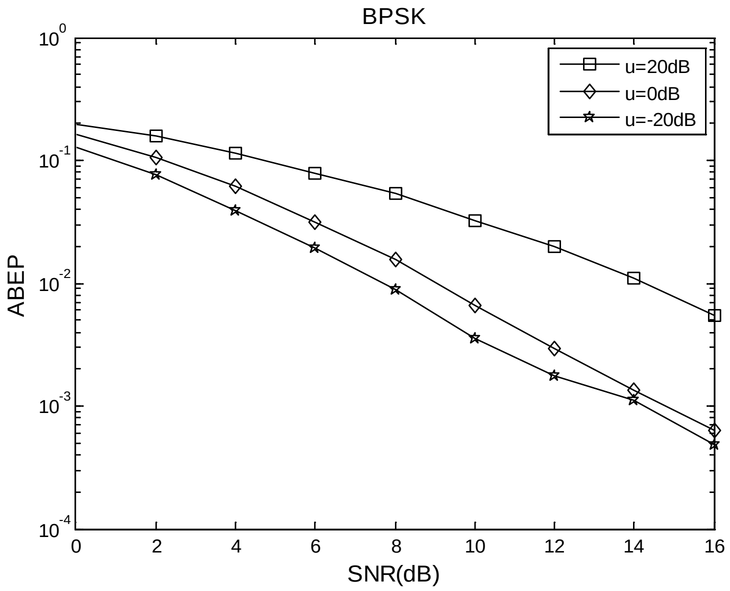

Fig. 4. The ABEP performance versus μ

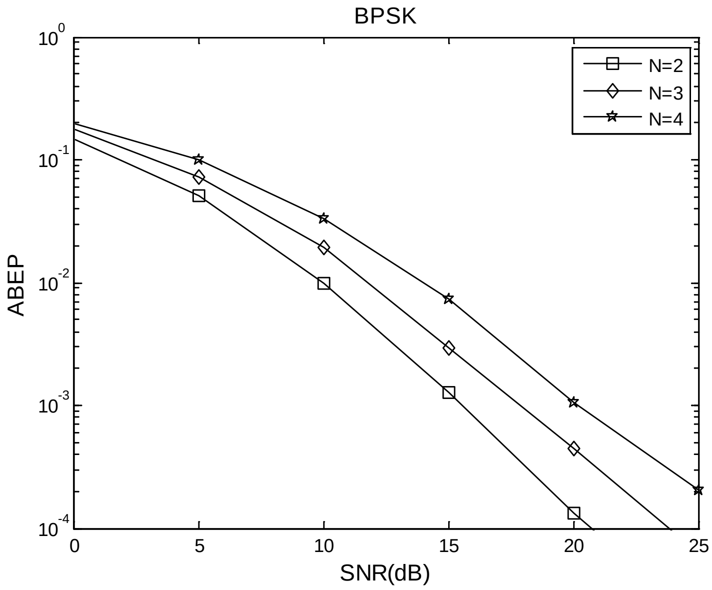

Fig. 5. The ABEP performance versus N

Fig. 4 presents the ABEP performance versus μ .The parameters are N=2, m=2, μ=20 dB, 0 dB,−20 dB,γ_t=4 dB, γ_p=2 dB,K=0.6. From **Fig. 4**, we can obtain that the ABEP performance for a lower μ outperforms the one for a higher μ. For example, when SNR=10 dB, μ=20 dB, the ABEP is 4×10^{-2}, μ=0 dB, the ABEP is 8×10^{-3}, μ=−20 dB, the ABEP is 5×10^{-3}. We can obtain that the best location for MR is near the MD. With the increase of SNR, the ABEP between them is reduced gradually.

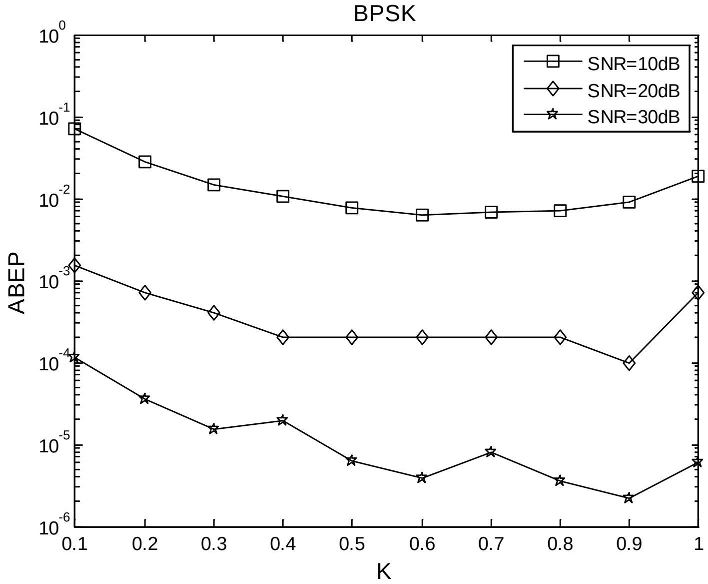

Fig. 6. The ABEP performance versus *K*

Fig. 5 presents the ABEP performance versus *N*. The parameters are *N*=2, 3, 4, *m*=2, μ=0 dB, γ_t=4 dB, γ_p=2 dB, *K*=0.9.From **Fig. 5**, we can obtain that the ABEP performance for a lower *N* outperforms the one for a higher *N*. For example, when SNR=15 dB, *N*=2, the ABEP is 1×10^{-3}, *N*=3, the ABEP is 3×10^{-3}, *N*=4, the ABEP is 7.5×10^{-3}.Increasing *N* means that the fading severity of the cascaded channels increases. With *N* fixed, increasing the SNR reduces ABEP gradually.

Fig. 6 presents the ABEP performance versus *K* . The parameters are *N*=2, *m*=2, μ=0 dB, γ_t=4 dB, γ_p=2 dB. As SNR increased, we can obtain that the ABEP performance is improved. For example, when *K*=0.6, the ABEP is 6×10^{-3} with SNR=10 dB, 2×10^{-4} with SNR=20 dB, 3.5×10^{-6} with SNR=30 dB. When SNR=10 dB, *K* = 0.69; SNR=20 dB, *K* = 0.87; SNR=30 dB, *K*= 0.97. We can conclude that *K*= 0.5,namely equal power allocation (EPA) scheme, is not the best scheme.

In **Table 2**, we present optimum values of *K* with BPSK and QPSK modulations. The parameters are *N*=2, *m*=2, μ=−5 dB,γ_t=2 dB, γ_p=0 dB.

Fig. 7 presents the ABEP performance versus EPA and optimum power allocation (OPA). For OPA, the values of *K* are used in Table 1 for BPSK modulation. For EPA, *K*=0.5. These results show that the ABEP performance of OPA is better than that of EPA. For example, with SNR=15 dB, the ABEP is 1.7×10^{-3} for OPA, while 3×10^{-3} for EPA.

Table 2. OPA parameters *K*

SNR	BPSK	QPSK
5	0.79	0.84
10	0.84	0.86
15	0.85	0.86
20	0.78	0.88
25	0.90	0.90
30	0.87	0.87

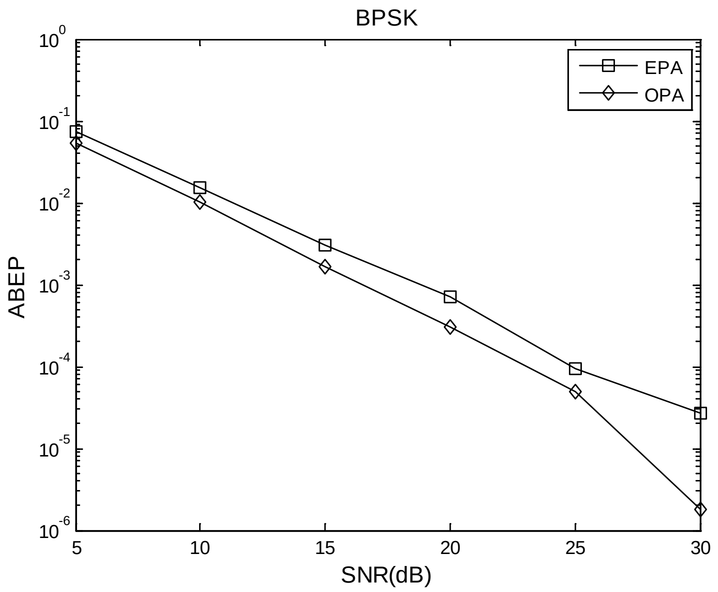

Fig. 7. The ABEP performance versus EPA and OPA

5. Conclusion

In this paper, we derive the exact ABEP expressions for M2M cooperative networks with the ISDF relaying.The simulation results show that the ABEP performance is affected by the parameters m, N, μ, and K. The expressions were derived which can be used to evaluate the ABEP performance of various practical application scenarios.

References

[1] H.J. Zhang, C. Jiang, J. Cheng, and V. C.M. Leung, "Cooperative interference mitigation and handover management for heterogeneous cloud small cell networks," *IEEE Wireless Communications*, vol. 22, no. 3, pp. 92-99, March,2015.Article (CrossRef Link)

[2] S. Mumtaz, K. M. Saidul Huq, and J. Rodriguez. "Direct mobile-to-mobile communication: Paradigm for 5G," *IEEE Wireless Communications*, vol. 21, no. 5, pp. 14-23, May,2014. Article (CrossRef Link)

[3] M. Jo, T. Maksymyuk, B. Strykhalyuk, C.H. Cho, "Device-to-device based heterogeneous radio access network architecture for mobile cloud computing," *IEEE Wireless Communications*, vol. 22, no. 3, pp. 50-58, March,2015.Article (CrossRef Link)

[4] J. Salo, H. E. Sallabi, and P. Vainikainen, "Statistical analysis of the multiple scattering radio channel," *IEEE Transactions on Antennas and Propagation*, vol. 54, no. 11, pp. 3114-3124, November, 2006.Article (CrossRef Link)

[5] B. Talha and M. Patzold, "Channel models for mobile-to-mobile cooperative communication systems: A state of the art review," *IEEE Vehicular Technology Magazine*, vol. 6, no.2, pp. 33-43, February, 2011.Article (CrossRef Link)

[6] P. M. Shankar, "Diversity in cascaded in N*Nakagami fading channels," *Annals of telecommunications*, vol. 68, no. 7, pp. 477-483, July, 2012.Article (CrossRef Link)

[7] M. Seyfi, S. Muhaidat, J. Liang, and M. Uysal, "Relay selection in dual-hop vehicular networks," *IEEE Signal Processing Letters*, vol. 18, no. 2, pp. 134-137, February, 2011. Article (CrossRef Link)

[8] F.K.Gong, J.Ge, and N. Zhang, "SER analysis of the mobile-relay-based M2M communication over double Nakagami-m fading channels," *IEEE Communications Letters*, vol. 15, no. 1, pp. 34-36, January , 2011. Article (CrossRef Link)
[9] G. K. Karagiannidis, N. C. Sagias, and P. T. Mathiopoulos. "N*Nakagami: A novel stochastic model for cascaded fading channels," *IEEE Transactions on Communications*, vol. 55, no. 8, pp. 1453-1458, August, 2007.Article (CrossRef Link)
[10] J.J. Wang, L.W. Xu, X.L. Dong, W. Shi, Q.N. Niu, "Performance analysis of M2M sensor networks," *International Journal of Distributed Sensor Networks*, Volume 2016, Article ID 8495097, 5 pages, 2016.Article (CrossRef Link)
[11] L.W. Xu, H. Zhang, J.J. Wang, and T. A. Gulliver. "Performance analysis of the double-antenna SDC system over *N*-Nakagami fading channels," *International Journal of Wireless Information Networks*, vol. 23, no. 1, pp. 49-56, January, 2016.Article (CrossRef Link)
[12] H. Ilhan, M. Uysal, and I. Altunbas, "Cooperative diversity for intervehicular communication: performance analysis and optimization," *IEEE Transactions on Vehicular Technology*, vol. 58, no. 7, pp. 3301-3310, July,2009.Article (CrossRef Link)
[13] L.W. Xu, H. Zhang, J.J. Wang, W. Shi, and T. A. Gulliver. "End-to-end performance analysis of AF relaying M2M cooperative system," *International Journal of Multimedia and Ubiquitous Engineering*, vol. 10, no. 9, pp. 211-224, September , 2015.Article (CrossRef Link)
[14] L.W. Xu, H. Zhang, and T. A. Gulliver. "Performance analysis of IDF relaying M2M cooperative networks over *N*-Nakagami fading channels," *KSII Transactions on Internet & Information Systems*, vol. 9, no. 10, pp. 3983-4001, October, 2015.Article (CrossRef Link)
[15] L.W. Xu, and H. Zhang, "Performance analysis of threshold digital relaying M2M cooperative networks," *Wireless Networks*, vol. 22, no. 5, pp. 1595-1603, May, 2016.Article (CrossRef Link)
[16] L.W. Xu, H. Zhang, T.T.Lu, and T. A. Gulliver. "Performance analysis of IAF relaying M2M cooperative networks over *N*-Nakagami fading channels," *Journal of Communications*, vol. 10, no. 3, pp.185-191, March,2015.Article (CrossRef Link)
[17] L.W. Xu, J.J.Wang, H. Zhang, and T. A. Gulliver. "Performance analysis of IAF relaying mobile D2D cooperative networks," *Journal of the Franklin Institute*, October, 2016. Article (CrossRef Link)
[18] L.W. Xu, H. Zhang, and T. A. Gulliver. "Performance analysis of SNR-Based HDAF M2M cooperative networks over *N*-Nakagami fading channels," *Journal of Electrical and Computer Engineering* , Volume 2015, Article ID 841937, 7 pages ,2015.Article (CrossRef Link)
[19] L.W. Xu, H. Zhang, and T. A. Gulliver. "Relay selection in the DF relaying M2M cooperative networks," *International Journal of Future Generation Communication and Networking* , vol. 9, no. 1, pp. 233-246, January, 2016.Article (CrossRef Link)
[20] L.W. Xu, H. Zhang, and T. A. Gulliver. "Joint TAS and power allocation for IHDAF relaying M2M cooperative networks," *KSII Transactions on Internet & Information Systems* , vol. 10, no. 5, pp. 1957-1975, May, 2016.Article (CrossRef Link)
[21] L.W. Xu, H. Zhang, T.T.Lu, and T. A. Gulliver. "Performance analysis of the SIR M2M cooperative networks," *International Journal of Control and Automation*, vol. 8, no. 5, pp. 407-416, May, 2015.Article (CrossRef Link)
[22] L.W. Xu, H. Zhang, T.T. Lu and T. A. Gulliver. "Outage probability analysis of the VAF relaying M2M networks," *International Journal of Hybrid Information Technology*, vol. 8, no.5, pp. 357-366, May, 2015. Article (CrossRef Link)
[23] L.W. Xu, H. Zhang, T.T. Lu and T. A. Gulliver. "Performance analysis of the home M2M cooperative networks," *International Journal of Smart Home*, vol. 9, no. 4, pp. 135-144, April, 2015.Article (CrossRef Link)
[24] H. Ochiai, P. Mitran, and V. Tarokh, "Variable-rate two-phase collaborative communication protocols for wireless networks," *IEEE Transactions on Vehicular Technology*, vol. 52, no. 9, pp. 4299-4313, September, 2006.Article (CrossRef Link)

[25] H. Chen, J. Liu, C. Zhai, Y.X. Liu, "Performance of Incremental-Selective Decode-and-Forward Relaying Cooperative Communications over Rayleigh Fading Channels," in *Proc. of Wireless Communications & Signal Processing*, pp. 1-5, November 13-15, 2009.Article (CrossRef Link)
[26] V. S. Adamchik, O. I. Marichev, "The algorithm for calculating integrals of hypergeometric type functions and its realization in reduce system," in *Proc. of International Conference on Symbolic and Algebraic Computation*, pp. 212-224, August 3-5,1990.Article (CrossRef Link)
[27] I. S. Gradshteyn, I. M. Ryzhik, "Table of integrals, series, and products," 5th edition. San Diego, CA: Academic, 1994.Article (CrossRef Link)
[28] G.F. Pan, E. Ekici, and Q.Y. Feng, "BER analysis of threshold digital relaying schemes over Log-Normal fading channels," *IEEE Communications Letters*, vol. 15, no.7, pp. 731-733, July, 2011. Article (CrossRef Link)

Lingwei Xu received his B.E. degree in Communication Engineering from Qingdao Technological University, P.R. China in 2011. He received his M.E. degree in Electronics and Communication Engineering from Ocean University of China, P.R. China in 2013 and his Ph.D. degree from Ocean University of China in 2016. Now, he is a lecturer in Qingdao University of Science & Technology. His research interests include ultra-wideband radio systems, MIMO wireless systems, and M2M wireless communications.

Jingjing Wang received the B.S. degree in Industrial Automation from Shandong University, China, in 1997, the M.Sc. degree in Control Theory and Control Engineering from Qingdao University of Science and Technology, China, in 2002, and the Ph.D. degree in Computer Application Technology from Ocean University of China, China, in 2012. Since 2002, she has been an Associate Professor in the College of Information Science and Technology, Qingdao University of Science and Technology. From 2014 to 2015, she was a visiting professor at the University of British Columbia. Her research interests include 60 GHz wireless communications, 60 GHz wireless positioning technology, UWB, MIMO wireless communications, M2M wireless communications and cooperative communication networks.

Han Wang received his B.S. degree in electrical engineering from Hubei University of Nationalities, China, in 2009 and the M.S. degree in information and communication system from Hainan University, Haikou, China, in 2013. He has worked in China Mobile Jiangxi branch as a network engineer for one year. Now, he is pursuing the Ph.D. degree with the Department of College of Information Science & Technology in Hainan University. His research interests include maritime communications and information theory.

T. Aaron Gulliver received his Ph.D. degree in Electrical and Computer Engineering from the University of Victoria, Victoria, BC, Canada in 1989. He is a professor in the Department of Electrical and Computer Engineering. From 1989 to 1991 he was employed as a Defense Scientist at Defense Research Establishment Ottawa, Ottawa, ON, Canada. He has held academic positions at Carleton University, Ottawa, and the University of Canterbury, Christchurch, New Zealand. He joined the University of Victoria in 1999 and is a Professor in the Department of Electrical and Computer Engineering. In 2002 he became a Fellow of the Engineering Institute of Canada, and in 2012 a Fellow of the Canadian Academy of Engineering. He is also a senior member of IEEE. His research interests include information theory and communication theory, and ultra wideband communication.